AD_____

AWARD NUMBER: W81XWH-16-1-0158

TITLE: Defining Hepatocellular Carcinoma Subtypes and Treatment Responses in Patient-Derived Tumorgrafts

PRINCIPAL INVESTIGATOR: Akbar Waljee, MD, MSc

RECIPIENT: University of Michigan
Ann Arbor, MI 48105

REPORT DATE: Oct 2019

TYPE OF REPORT: Annual

PREPARED FOR: U.S. Army Medical Research and Materiel Command
Fort Detrick, Maryland 21702-5012

REPORT DOCUMENTATION PAGE

Form Approved
OMB No. 0704-0188

1. REPORT DATE	2. REPORT TYPE	3. DATES COVERED
Oct 2019	Annual	30 Sept 2018-29 Sept 2019

4. TITLE AND SUBTITLE
Defining hepatocellular carcinoma subtypes and treatment responses in patient derived tumorgrafts

5a. CONTRACT NUMBER

5b. GRANT NUMBER
W81XWH-16-1-0158

5c. PROGRAM ELEMENT NUMBER

6. AUTHOR(S)
Hao Zhu, Amit Singal, Adam Yopp, Daniel Siegwart, Akbar Waljee

E-Mail: amit.singal@utsouthwestern.edu; awaljee@med.umich.edu

5d. PROJECT NUMBER

5e. TASK NUMBER

5f. WORK UNIT NUMBER

7. PERFORMING ORGANIZATION NAME(S) AND ADDRESS(ES)

UT Southwestern Medical Center
5323 Harry Hines Blvd.
Dallas, TX 75390-9020

Veteran's Education and Research Association of Michigan (VERAM)
2215 Fuller Rd Rear
Ann Arbor, MI 48105-23032

8. PERFORMING ORGANIZATION REPORT NUMBER

9. SPONSORING / MONITORING AGENCY NAME(S) AND ADDRESS(ES)

U.S. Army Medical Research and Materiel Command
Fort Detrick, Maryland 21702-5012

10. SPONSOR/MONITOR'S ACRONYM(S)

11. SPONSOR/MONITOR'S REPORT NUMBER(S)

12. DISTRIBUTION / AVAILABILITY STATEMENT

Approved for Public Release; Distribution Unlimited

13. SUPPLEMENTARY NOTES

14. ABSTRACT
Hepatocellular carcinoma (HCC) is the 6th most common cancer and 3rd leading cause of cancer-related death worldwide. We know that HCC subtypes exist because clear clinical, radiographic, and histological differences between patients with HCC are observed. In this study we proposed to investigate distinct subtypes of HCC using a mouse-human chimeric Patient Derived Xenograft (PDX) approach. So far, we have performed a large effort to implant 102 tumors from human HCC patients from Texas. We have established the protocol and the results have taught us that engraftment using a variety of transplantation techniques will result in a 25-30% engraftment efficiency for early stage surgical tumors. We have established 6 new human HCC PDX models that will be highly relevant for therapeutic and biological studies. These represent North American HCCs, including some patients with intermediate/advanced stage HCC, which is a unique resource for the field.

15. SUBJECT TERMS
HCC, patient derived xenografts, siRNA, mouse models of cancer.

16. SECURITY CLASSIFICATION OF:			17. LIMITATION OF ABSTRACT	18. NUMBER OF PAGES	19a. NAME OF RESPONSIBLE PERSON
a. REPORT	b. ABSTRACT	c. THIS PAGE			USAMRMC
Unclassified	Unclassified	Unclassified	Unclassified	28	19b. TELEPHONE NUMBER *(include area code)*

Standard Form 298 (Rev. 8-98)
Prescribed by ANSI Std. Z39.18

TABLE OF CONTENTS

1. **INTRODUCTION:** Narrative that briefly (one paragraph) describes the subject, purpose and scope of the research.

Hepatocellular carcinoma (HCC) is the 6th most common cancer and 3rd leading cause of cancer-related death worldwide. In the US, its incidence has doubled over the past two decades due to the growing number of patients with hepatitis C virus (HCV) and/or non-alcoholic steatohepatitis (NASH) (El-Serag, 2004, 2012). We know that HCC subtypes exist because clear clinical, radiographic, and histological differences between patients with HCC are observed (Yopp et al., 2015). In this study we proposed to investigate distinct subtypes of HCC using a mouse-human chimeric Patient Derived Xenograft (PDX) approach. We aim to analyze and functionalize early and advanced stage HCC tumors with a large and representative cohort of patient derived xenograft (PDX) models. Our hypothesis is that HCC is poorly understood because tissue has been obtained from early HCC but not advanced cases. Biological subclasses of HCCs that behave differently in terms of natural history, prognosis and treatment response have not been categorized and/or functionally analyzed. Our team will use human-mouse PDX models to uncover novel biology and establish a platform to study experimental therapeutics.

2. **KEYWORDS:** Provide a brief list of keywords (limit to 20 words).

HCC, patient derived xenografts, siRNA, mouse models of cancer.

3. **ACCOMPLISHMENTS:** The PI is reminded that the recipient organization is required to obtain prior written approval from the awarding agency Grants Officer whenever there are significant changes in the project or its direction.

What were the major goals of the project?
For reference, the complete Statement of Work (SOW) is presented below with detail of Aims, Major Tasks, and Subtasks with Anticipated time lines. The column titled “Progress” indicates portion of the Major Task and related Sub-tasks completed.

Site 1:	UT Southwestern Medical Center	**Site 2:**	Ann Arbor Veterans Affairs Healthcare System
	5323 Harry Hines Blvd		2215 Fuller Rd
	Dallas, TX 75390		Ann Arbor, MI 48105
	Initiating PI: Dr. Hao Zhu Partnering PIs: Drs. Amit Singal; Adam Yopp; Daniel Siegwart		Partnering PI: Dr. Waljee

Specific AIM 1: Determine if early vs. advanced HCCs have distinct cell-intrinsic biology in PDX engraftment assays	**Timeline in months**	**Site 1** (Initiating PI)	**Site 2** (Partnering PI)	**Progress (*Percent Complete or Completion Date***
Major Task 1: Expand and characterize PDX models derived from surgical and biopsy HCC specimens				
Pre-task: Allow time to receive the regulatory approval for animal use (IACUC and DoD ACURO)	1-3	Drs. Yopp, Singal, and Zhu		100 % complete November 2016
Pre-task 2: Allow time to receive the regulatory approval for the Human Anatomical Substance use (IRB and DoD HRPO).	1-3	Drs. Yopp, Singal, and Zhu		100 % complete November 2016
Subtask 1: Continue to implant 40 surgical HCC specimens in the subcutaneous space and livers of NSG mice	0-12	Drs. Yopp and Zhu		100% complete Sep 2018
Subtask 2: Continue to implant 25 biopsy samples from intermediate and advanced HCC cases in the subcutaneous space and livers of NSG mice	0-12	Drs. Yopp, Singal, and Zhu		100% complete Sep 2018
Subtask 3: Harvest primary PDX tumors, establish PDX bank, and passage into additional NSG mice	6-18	Drs. Yopp and Zhu		100% complete Oct 2018
Subtask 4: Characterize tumor architecture, histology, growth, invasiveness, and paraneoplastic features of tumors that engraft, and determine if the grafts resemble or deviate from original tumors (surgical or biopsy specimens)	6-24	Drs. Yopp and Zhu		100% complete Sept 2018
Subtask 5: Obtain genomic data from PDX grafts to determine if they resemble or deviate from original tumors (surgical or biopsy specimens)	12-30	Drs. Yopp, Singal, and Zhu		100% complete June 2018
Major Task 2: Compare biological and genetic features (stage, survival, progression) of early vs. non-early HCCs				
Subtask 1: Compare biological features of the tumors that engraft vs. those that do not, and determine if there is a difference between PDX made from early surgical or more advanced biopsy specimens	6-24	Drs. Yopp and Zhu		100% complete April 2019

Subtask 2: Compare patient clinical features (stage, survival, progression) of specimens that engraft versus not engraft and determine if engraftment can predict clinical outcomes	6-18	Drs. Singal,	Drs. Wajlee	100% complete October 2018
Subtask 3: Analyze genomic data to survey genetic landscape of PDX population that successfully engrafts and identify genetic drivers of engraftment	12-36	Drs. Singal and Zhu	Drs. Wajlee	100% complete October 2018
Milestone #1: Co-author manuscript on biology and genomics of HCC PDX models	12-24	Drs. Zhu, Singal, and Yopp	Drs. Wajlee	100% complete July 2019
Specific AIM 2: Determine the efficacy of small RNA therapeutics against the *LIN28B/LET-7* pathway in PDXs activating this oncogenic pathway	**Timeline**	**Site 1** (Initiating PI)	**Site 2** (Partnering PI)	
Major Task 1: Identify and deliver small RNAs to target PDX populations				
Subtask 1: Evaluate and optimize custom dendritic nanoparticle delivery to PDX tumors	0-12	Drs. Zhu and Siegwart		100% complete Dec 2018
Subtask 2: Formulate and optimize siRNA and microRNA containing dendritic nanoparticles to ensure that successful modulation of LIN28B and or LET-7 is achieved in PDX models.	6-24	Dr. Siegwart		100% Sept 2019
Subtask 3: Define HCC PDX models that overexpress MYC or LIN28B and those that suppress LET-7 family microRNAs	6-24	Drs. Singal and Zhu		Incomplete, discontinued
Subtask 4: Therapeutically deliver siRNAs or microRNAs in dendritic nanoparticles to mice harboring these PDX models	12-36	Dr. Siegwart		20% complete July 2019
Major Task 3: Define response to small RNAs in target PDX populations				
Subtask 1: Determine response to small RNA therapies using luciferase and CT imaging	6-30	Dr. Siegwart		50% complete (performed in analogous models)
Subtask 2: Define histological response and intermediate markers of tumor biology (Ki67, apoptosis, necrosis)	12-36	Dr. Siegwart		50% complete (performed in analogous models)

Milestone #2: Co-author manuscript about therapeutic efficacy of small RNA therapy in HCC PDX models	24-36	Drs. Zhu and Siegwart		Not completed
Specific AIM 3: Define targeted therapy responders with HCC-PDX patient avatars and use to identify predictive biomarkers	**Timeline**	**Site 1** (Initiating PI)	**Site 2** (Partnering PI)	
Major Task 1: Define PDX models that show partial response, stable disease, and progressive disease to targeted therapies				
Subtask 1: Characterize tumors for growth, histology, vascular invasion, metastasis, proliferation and apoptosis after treatment	12-36	Drs. Zhu, Yopp, and Singal		100% complete Oct 2018
Subtask 2: Perform exome and RNA-expression sequencing for top responders and non-responders for each group to determine mechanistic basis of response	18-36	Drs. Singal and Zhu	Dr. Waljee	100% complete July 2019
Major Task 2: Establish predictive biomarkers for response to treatment				
Subtask 1: Use machine learning methods to identify clinical and genetic factors associated with response to targeted therapies	18-36	Drs. Yopp, and Singal	Dr. Waljee	100% complete Oct 2018
Subtask 2: Derive and internally validate predictive model using factors significantly associated with targeted therapy response	24-36	Dr. Singal	Dr. Waljee	30% complete July 2019
Milestone #3: Co-author manuscript on HCC PDX treatments and predictive modeling results	24-36	Drs. Zhu, Yopp, and Singal	Dr. Waljee	50% complete July 2019

What was accomplished under these goals?

Specific AIM 1: Determine if early vs. advanced HCCs have distinct cell-intrinsic biology in PDX engraftment assays
Major Task 1: Expand and characterize PDX models derived from surgical and biopsy HCC specimens
Subtask 1: Implant surgical HCC specimens in the subcutaneous space and livers of NSG mice. This task has been completed.
Subtask 2: Continue to implant 25 biopsy samples from intermediate and advanced HCC cases in the subcutaneous space and livers of NSG mice. This subtask has been completed.
Subtask 3: Harvest primary PDX tumors, establish PDX bank, and passage into additional NSG mice. This task has been completed. We also thawed some PDX lines and found that most of the lines can be thawed from frozen stock and grow. Altogether we found that among 9 lines of

transplantable PDXs, 7 lines can be thawed and re-grown in mice. These lines are HS-84, HS-127, HS-131, HS-157, HS-119, HB-163, and HB-179. This makes it possible to stock the PDX lines in a bank and use them later to test therapies without constantly maintaining the lines in live mice. When thawed, the PDX lines can also be passaged and still maintain the histology of the patient tumors (Figure A & B). For HS-141, although we were not able to thaw the frozen stock successfully, the primary PDX tumor of HS-141 has been successfully passaged for 7 times and are still growing. Thus, 8 total lines can be used for drug testing. We will test the histology of the PDXs after multiple passages to see whether these PDXs still represent the patient tumor and maintain the biological features of their parent patient tumors.

Subtask 4: Characterize tumor architecture, histology, growth, invasiveness, and paraneoplastic features of tumors that engraft, and determine if the grafts resemble or deviate from original tumors (surgical or biopsy specimens).

This subtask is complete.

Subtask 5: Obtain genomic data from PDX grafts to determine if they resemble or deviate from original tumors (surgical or biopsy specimens).

This has been completed and analyzed in a more detailed way. Here we showed that the HCC PDXs retain the genomic expression and mutational profiles of parental tumors. A. Principal component analysis (PCA) of RNA-seq data from 7 pairs of parental tumors and PDX samples showed conservation of gene expression and B. We also performed hierarchical clustering of samples based on evaluation of highly expressed genes in HCC. C. Whole-exome sequencing in parental tumors and PDX models generally showed preservation of mutated genes. D. Oncoplot of mutations in parental tumors and PDXs. We focused on 35 genes commonly mutated genes in HCC based on the TCGA analysis. COSMIC mutations or exome mutations compared to 1000 genomes are shown. See below Figure.

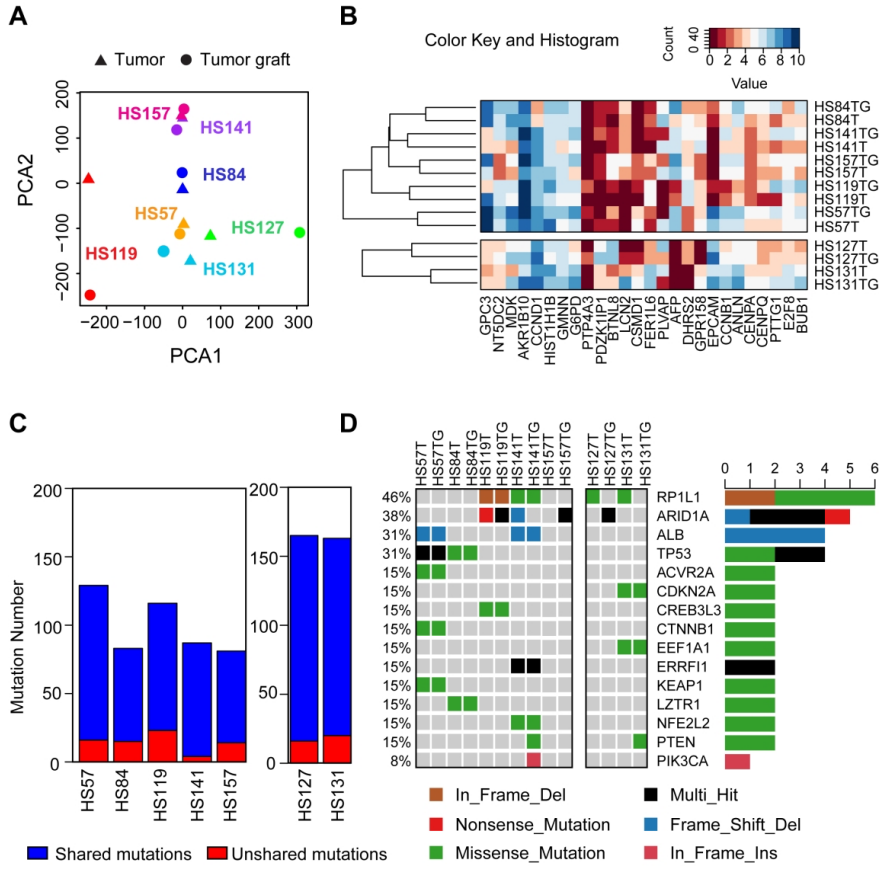

Major Task 2: Compare biological and genetic features (stage, survival, progression) of early vs. non-early HCCs

Subtask 1: Compare biological features of the tumors that engraft vs. those that do not, and determine if there is a difference between PDX made from early surgical or more advanced biopsy specimens

This has been completed under the supervision of Drs. Yopp, Singal, and Zhu.

Subtask 2: Compare patient clinical features (stage, survival, progression) of specimens that engraft versus not engraft and determine if engraftment can predict clinical outcomes

Dr. Waljee's team performed explanatory analyses to find association between PDX engraftment results and several clinical features. We aimed to determine if clinical variables such as tumor differentiation correlated with engraftment. Among 69 surgical HCC cases, 43 cases were moderately differentiated and 9 of these successfully engrafted (21%, see Supplementary Table 2). Seventeen were poorly differentiated and 5 engrafted (29%). When comparing the engraftment for "moderate", "moderate to poor", and "poor" HCCs, there was a non-significant trend of increasing engraftment from 21% to 25% to 29%. However, 3/17 poorly differentiated HCCs were serially transplantable while 0/43 moderately differentiated HCCs were transplantable (Fisher's exact test p=0.02). Surprisingly, the well differentiated HCC samples could also engraft, although the number of cases was not high enough to evaluate the engraftment rate. Previous reports of Asian HCC PDX models showed that engraftment correlated with tumor cell proliferation as measured by Ki-67. In our cohort, Ki-67 staining on 20 engrafting and 37 non-engrafting primary tumors showed no significant differences in the frequency of Ki-67 positive cells. In addition, clinical features such as ALT, AST, and sodium levels could not predict engraftment (data not shown). We think additional predictors are going to be difficult to find unless we have a much larger number of engrafting tumors. This task has been completed.

Subtask 3: Analyze genomic data to survey genetic landscape of PDX population that successfully engrafts and identify genetic drivers of engraftment

Dr. Waljee's team considered a variety of gene selection methods, including (1) logistic regression model with lasso regularization, (2) logistic regression model with elastic net regularization, (3) nearest shrunken centroid (NSC) method, and (4) adaptive hierarchically penalized NSC (AHP-NSC). The results are shown in table 1. The logistic regression model with lasso penalty method resulted in the highest accuracy rate of 76%. We also identified several genes that can potentially drive engraftment: SNORD15B; SNORA53; RP11−182J1.5; ZNF205; CX3CL1; RP5−837J1.1; MFSD9; SCARNA5; RAB3B.

Method	Accuracy rate
(1) logistic regression model with lasso	0.76
(2) logistic regression model with elastic net	0.74
(3) NSC	0.60
(4) AHP-NSC	0.64

We further studied how genomic data can predict engraftment by taking three important known clinical confounders into consideration. None of the three clinical confounders were not selected in our models for prediction. This may be due to small sample size. To determine if we could identify transcriptomic predictors of engraftment, we also performed deep RNA-seq on cohorts of parental tumors that either did or did not engraft in PDX assays (n = 17 and 19). However, we did not find

gene sets that could distinguish between engrafting and non-engrafting cases using gene set enrichment analysis (GSEA). This task is complete.

Milestone #1: Co-author manuscript on biology and genomics of HCC PDX models
The manuscript has been favorably reviewed and is in 2nd review at Hepatology.

Specific AIM 2 (Determine the efficacy of small RNA therapeutics against the LIN28B/LET-7 pathway in PDXs activating this oncogenic pathway).

Major Task 1: Identify and deliver small RNAs to target PDX populations

Subtask 1: Evaluate and optimize custom dendritic nanoparticle delivery to PDX tumors
This has been completed.

Subtask 2: Formulate and optimize siRNA and microRNA containing dendritic nanoparticles to ensure that successful modulation of LIN28B and or LET-7 is achieved in PDX models.
This has been completed.

Subtask 3: Define HCC PDX models that overexpress MYC or LIN28B and those that suppress LET-7 family microRNAs
We did not find any PDXs that were overexpressing LIN28B, thus we have altered the targets for this subtask. Instead we will use an siRNA to target ANLN, which is a gene required for cytokinesis. We have previously shown in other work that this is a good therapeutic target for liver cancer.

Subtask 4: Therapeutically deliver siRNAs or microRNAs in dendritic nanoparticles to mice harboring these PDX models
In our previous report, we described our discovery of hepatocyte-specific and Kuppfer cell-specific dendrimer lipid nanoparticles (DLNPs). We made the exciting observation that dendrimer chemistry can control cellular tropism within the liver. Fortunately, the previously selected and validated carrier (5A2-SC8 dendrimer lipid nanoparticles (DLNPs)) with which we have obtained all prior tumor cell data continued to show efficacy in these new experiments. Thus, when comparing 5A2-SC8 DLNPs to 3A5-SC8 DLNPs, we found that 5A2-SC8 DLNPs continue to be ideal for carrying out the funded cancer studies.

We showed that 5A2-SC8 DLNPs can target cancer cells and hepatocytes in the liver, while 3A5-SC8 DLNPs instead target Kupffer cells. Building on this research, we have further confirmed these effects on the cellular level.

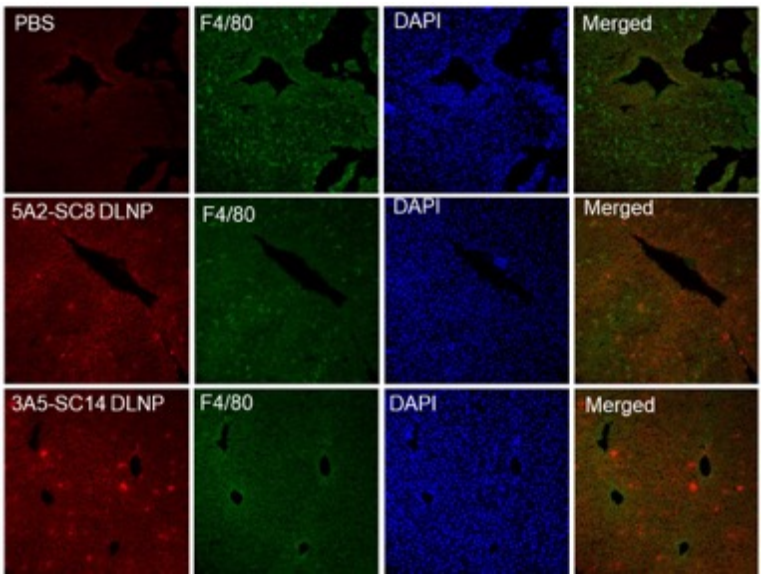

The above Figure shows differential uptake of DLNPs in the liver after delivery of siRNA-Cy5.5. Our previous data (from the last quarter report) was further confirmed. When we deleted Kuppfer cells in the liver, now the biodistribution of 3A5-SC8 DLNPs was significantly altered.

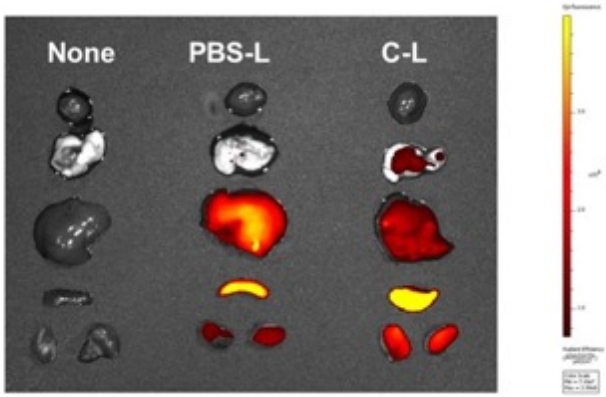

Depletion of Kupffer cells alters 3A5-SC14 DLNP biodistribution (3A5-SC14 DLNP 0.5 mg/kg siFVII-Cy5.5, 6 hours) from the liver Kuppfer cells to liver hepatocytes and splenic macrophages. This knowledge is continuing to aid our investigations of cancer therapy in PDX models. We have further expanded our models and nanoparticles in this past period.

Major Task 3: Define response to small RNAs in target PDX populations

Subtask 1: Determine response to small RNA therapies using luciferase and CT imaging
Drs. Zhu, Yopp, and Siegwart are working on this now during the NCE period.

Subtask 2: Define histological response and intermediate markers of tumor biology (Ki67, apoptosis, necrosis)
To be completed after initiation of the small RNA therapeutics nanoparticle studies. We have obtained ANLN siRNAs from Alnylam to perform these experiments.

Specific AIM 3: Define targeted therapy responders with HCC-PDX patient avatars and use to identify predictive biomarkers

Major Task 1: Define PDX models that show partial response, stable disease, and progressive disease to targeted therapies

Subtask 1: Characterize tumors for growth, histology, vascular invasion, metastasis, proliferation and apoptosis after treatment
We have performed selected drug studies in the PDX models so this has been completed. We have also started testing experimental drugs that target telomere elongation. This is a drug developed by Jerry Shay at UTSW. So far, some PDXs have not responded to these drugs but we are continuing to add more PDX models to the testing scheme.

Subtask 2: Perform exome and RNA-expression sequencing for top responders and non-responders for each group to determine mechanistic basis of response
This has not been completed because the numbers of PDXs and therefore responder/non-responder cohorts are too small for this type of analysis.

Major Task 2: Establish predictive biomarkers for response to treatment

Subtask 1: Use machine learning methods to identify clinical and genetic factors associated with response to targeted therapies
This has not been completed because we do not have enough responders and non-responders.

Subtask 2: Derive and internally validate predictive model using factors significantly associated with targeted therapy response
This has not been completed and will be discontinued.

Milestone #3: Co-author manuscript on HCC PDX treatments and predictive modeling results
This has not been completed. Other work involving PDX models will be pursued and published.

What opportunities for training and professional development has the project provided?

Nothing to report during this period.

How were the results disseminated to communities of interest?

Nothing to report besides the paper that we have submitted to Hepatology.

What do you plan to do during the next reporting period to accomplish the goals?

For the small RNA parts of the grant, we will shift focus to Anln siRNA in the place of Lin28-let-7 because there are potentially more PDX models which express and depend on Anln, a cytokinesis protein that is essential for cancer growth. This would help us considerably with the completion of AIM 2. Our goal is to test human *ANLN* siRNAs in human HCC PDX models. We will functionally assess the ability of either siRNA approach to enter and treat early HCCs. Because our previous siRNAs were designed against mouse ANLN, we will use optimized human ANLN siRNAs screened by our collaborator Alnylam. We will test delivery and efficacy in the distinct HCC PDX models that we have made (Zhu et al, *Hepatology, manuscript in revision*) and that we will continue to generate in a prospective fashion. All tumors will be grown until at least 200 mm^3 and then mice will be dosed with IV LNP-siRNA. Tumor volume will be followed over a 3-5 week period using the formula volume = $width^2$ x length/2. Completion of this goal will open up additional therapeutic development opportunities.

For Specific AIM 3 (Define targeted therapy responders with HCC-PDX patient avatars and use predictive modeling to identify prognostic biomarkers), we plan to treat these PDX lines with other drugs, including WNT inhibitors and other inhibitors from our collaborators. This would be valuable information for the development of WNT inhibitors.

4. **IMPACT:** Describe distinctive contributions, major accomplishments, innovations, successes, or any change in practice or behavior that has come about as a result of the project relative to:

What was the impact on the development of the principal discipline(s) of the project?

The major impact at this point is that we have performed a large effort to implant 102 tumors from human HCC patients from Texas. We have established the protocol and the results have taught us how efficient this process will be. We have established 6 new human HCC PDX models that will be highly relevant for therapeutic and biological studies. These represent North American HCCs, including some patients with intermediate/advanced stage HCC, which is a unique resource for the field. We have found that increasing the rate of engraftment with partial hepatectomy or mouse models of chronic liver disease helps to make the growth and engraftment of the tumors more efficient. We will be able to use these models to evaluate experimental therapeutics, in the form of small molecules or small interfering RNAs.

What was the impact on other disciplines?

Nothing to report

What was the impact on technology transfer?

Nothing to report

What was the impact on society beyond science and technology?

Nothing to report

5. **CHANGES/PROBLEMS:** The Project Director/Principal Investigator (PD/PI) is reminded that the recipient organization is required to obtain prior written approval from the awarding agency Grants Officer whenever there are significant changes in the project or its direction. If not previously reported in writing, provide the following additional information or state, "Nothing to Report," if applicable:

Changes in approach and reasons for change

Nothing to report

Actual or anticipated problems or delays and actions or plans to resolve them

Nothing to report

Changes that had a significant impact on expenditures

Nothing to report

Significant changes in use or care of human subjects, vertebrate animals, biohazards, and/or select agents

Significant changes in use or care of human subjects

Nothing to report.

Significant changes in use or care of vertebrate animals.

None

Significant changes in use of biohazards and/or select agents

Nothing to report

6. PRODUCTS:

- **Publications, conference papers, and presentations**

  Report only the major publication(s) resulting from the work under this award.

  Journal publications.

  1. Zhu et al, Hepatology in revision.
  2. "Dendrimer-based lipid nanoparticles deliver therapeutic FAH mRNA to normalize liver function and extend survival in a mouse model of Hepatorenal Tyrosinemia Type I." Qiang Cheng, Tuo Wei, Yuemeng Jia, Lukas Farbiak, Kejin Zhou, Shuyuan Zhang, Yonglong Wei, Hao Zhu, and Daniel J. Siegwart.* Advanced Materials, 2018, 30, 1805308.

  Books or other non-periodical, one-time publications.

  Nothing to report

  Other publications, conference papers, and presentations.

  Nothing to report

- **Website(s) or other Internet site(s)**

Nothing to report

- **Technologies or techniques**

These techniques have been described above and will be reported to the community when a manuscript is published.

- **Inventions, patent applications, and/or licenses**

Nothing to report.

- **Other Products**

Data or databases: We continue to collect patient data in a clinical database.
Biospecimen collections: We have a human HCC biospecimen and PDX collection.
Research material: We have established live mice carrying human HCC PDXs.

7. PARTICIPANTS & OTHER COLLABORATING ORGANIZATIONS

What individuals have worked on the project?

Name: Hao Zhu
Project Role: Lead PI
Researcher Identifier (e.g. ORCID ID): 0000-0002-8417-9698
Nearest person month worked: 36
Contribution to Project: Direct the project, design the experiments and objectives, organize personnel, report progress to the DOD.

Name: Lin Li
Project Role: Senior Research Associate)
Researcher Identifier (e.g. ORCID ID): none
Nearest person month worked: 36
Contribution to Project: implantation of HCC specimens, passage of engrafted PDXs, storage of PDX engrafts.

Name: Daniel Siegwart
Project Role: Co-PI
Researcher Identifier (ORCID ID): 0000-0003-3823-1931
Nearest person month worked: 36
Contribution to Project: Co-planned and co-directed research activities. Worked on 5A2-SC8 synthesis and purification. Worked on nanoparticle delivery optimization to liver tumors.

Name: Qiang Cheng
Project Role: Senior Research Associate
Researcher Identifier (e.g. ORCID ID): none
Nearest person month worked: 36
Contribution to Project: Developed nanoparticle delivery carriers with an improved ability to deliver RNAs to the liver. Assisted with 5A2-SC8 experiments.

Name: Adam Yopp
Project Role: Co-PI
Researcher Identifier (e.g. ORCID ID):
Nearest person month worked: 36
Contribution to Project: Design and conducted experiments, participated in co-PI conference calls to organize personnel and direct project.

Name: Min Zhu
Project Role: Senior Research Associate
Researcher Identifier (e.g. ORCID ID): none
Nearest person month worked: 36
Contribution to Project: implantation of HCC specimens, passage of engrafted PDXs, storage of PDX engrafts. inventory of HCC samples, preparation of genomic DNA libraries from HCC samples, data analysis, etc.

Name: Amit Singal
Project Role: Co-PI
Researcher Identifier (e.g. ORCID ID): 0000-0002-1172-3971
Nearest person month worked: 36
Contribution to Project: Design experiments, participated in co-PI conference calls to organize personnel and direct project.

Name: Veronica Renteria
Project Role: Research coordinator
Researcher Identifier (e.g. ORCID ID): none
Nearest person month worked: 36
Contribution to Project: collection of HCC specimens

Name: Amanda Ellis
Project Role: Research assistant
Researcher Identifier (e.g. ORCID ID): N/A
Nearest person month worked: 2.4
Contribution to Project: Ms. Ellis has performed administrative duties such as organizing meetings, regulatory policies, and served as liaison between AAVA and UTSW.

Name: Xianshi Yu
Project Role: Statistician
Researcher Identifier (e.g. ORCID ID): N/A
Nearest person month worked: 1
Contribution to Project: Will be helping predict engraftment using both clinical and various predictor genes.

Has there been a change in the active other support of the PD/PI(s) or senior/key personnel

For Akbar Waljee, the following grant has become active:
UMHS-CGMH Waljee (Partner-PI) 06/01/2019-05/31/2020
Title: The genetic, environmental, and microbial determinant of IBD pathogenesis in Taiwan vs the U.S.
This joint project between CGMH and UMHS aims to better characterize IBD phenotypes and to identify potential risk factors by examining host genome, environmental exposures, and gut microbiota. Successful establishment of this pilot biorepository will provide the necessary preliminary data and available samples for an extramural grant application to perform more extensive analyses (e.g., host metatranscriptomics and serum metabolomics, fecal microbiota metagenomics/metatranscriptomics and metabolomics).

What other organizations were involved as partners?

Nothing to report

8. SPECIAL REPORTING REQUIREMENTS

COLLABORATIVE AWARDS: For collaborative awards, independent reports are required from BOTH the Initiating PI and the Collaborating/Partnering PI. A duplicative report is acceptable; however, tasks shall be clearly marked with the responsible PI and research site. A report shall be submitted to **https://ers.amedd.army.mil** for each unique award.

QUAD CHARTS: If applicable, the Quad Chart (available on https://www.usamraa.army.mil) should be updated and submitted with attachments.

9. APPENDICES: Attach all appendices that contain information that supplements, clarifies or supports the text. Examples include original copies of journal articles, reprints of manuscripts and abstracts, a curriculum vitae, patent applications, study questionnaires, and surveys, etc.

ADVANCED MATERIALS
www.advmat.de

Dendrimer-Based Lipid Nanoparticles Deliver Therapeutic FAH mRNA to Normalize Liver Function and Extend Survival in a Mouse Model of Hepatorenal Tyrosinemia Type I

*Qiang Cheng, Tuo Wei, Yuemeng Jia, Lukas Farbiak, Kejin Zhou, Shuyuan Zhang, Yonglong Wei, Hao Zhu, and Daniel J. Siegwart**

mRNA-mediated protein replacement represents a promising concept for the treatment of liver disorders. Children born with fumarylacetoacetate hydrolase (FAH) mutations suffer from Hepatorenal Tyrosinemia Type 1 (HT-1) resulting in renal dysfunction, liver failure, neurological impairments, and cancer. Protein replacement therapy using FAH mRNA offers tremendous potential to cure HT-1, but is currently hindered by the development of effective mRNA carriers that can function in diseased livers. Structure-guided, rational optimization of 5A2-SC8 mRNA-loaded dendrimer lipid nanoparticles (mDLNPs) increases delivery potency of FAH mRNA, resulting in functional FAH protein and sustained normalization of body weight and liver function in $FAH^{-/-}$ knockout mice. Optimization using luciferase mRNA produces DLNP carriers that are efficacious at mRNA doses as low as 0.05 mg kg^{-1} in vivo. mDLNPs transfect > 44% of all hepatocytes in the liver, yield high FAH protein levels (0.5 mg kg^{-1} mRNA), and are well tolerated in a knockout mouse model with compromised liver function. Genetically engineered $FAH^{-/-}$ mice treated with FAH mRNA mDLNPs have statistically equivalent levels of TBIL, ALT, and AST compared to wild type C57BL/6 mice and maintain normal weight throughout the month-long course of treatment. This study provides a framework for the rational optimization of LNPs to improve delivery of mRNA broadly and introduces a specific and viable DLNP carrier with translational potential to treat genetic diseases of the liver.

Hepatorenal tyrosinemia type I (HT-1) is devastating and fatal genetic disease that results in liver failure, renal dysfunction, neurological impairments, and cancer.[1] Mutations in fumarylacetoacetate hydrolase (FAH) prevent catalysis of the terminal step in the tyrosine catabolic pathway, causing an accumulation of toxic metabolites including succinylacetone that result in clinical HT-1 symptoms typically appearing before 6 months of age. HT-1 is currently treated with 2-(2-nitro-4-trifluoromethylbenzoyl)-1,3-cyclohexanedione (NTBC, nitisinone), which inhibits 4-hydroxyphenylpyruvate dioxygenase, the second step in the tyrosine catabolic pathway. This reduces the need for liver transplant, but comes with significant hepatic complications, only partially blocks the pathway, and does not eliminate the high risk of hepatocellular carcinoma (HCC). Messenger RNA (mRNA)-mediated FAH protein replacement therapy therefore offers tremendous therapeutic potential that would overcome the side effects of NTBC and simplify treatment over potential gene editing approaches that would be difficult to implement due to the large number of known mutations (about 100) in FAH.[1,2] Here we developed synthetic nanoparticles that effectively deliver FAH mRNA to restore normal liver function and extend survival in a difficult-to-treat, genetically engineered knockout mouse model of HT-1.

To date, gene therapy for HT-1 has been limited by the long-standing delivery challenge of safety transfecting large numbers of hepatocytes with high efficacy and safety across repeated dosing.[3] Adeno-associated virus (AAV) therapies remain promising, but have been associated with hepatic genotoxity in mice and repeat dosing is not effective due to production of neutralizing antibodies.[4] Recent efforts to develop non-viral delivery systems suggest feasibility to safely replace FAH. Still, challenges remain to implement nanocarriers for diseases afflicted by poor liver function, particularly because lipids and materials can exacerbate the underlying disease and abate efficacy.[5] Due to these challenges, there has not been any report to our knowledge of successful FAH mRNA treatments in lethal disease models of HT-1.

Dr. Q. Cheng, Dr. T. Wei, L. Farbiak, Dr. K. Zhou, Prof. D. J. Siegwart
Simmons Comprehensive Cancer Center
Department of Biochemistry
University of Texas Southwestern Medical Center
Dallas, TX 75390, USA
E-mail: Daniel.Siegwart@UTSouthwestern.edu
Y. Jia, Dr. S. Zhang, Dr. Y. Wei, Prof. H. Zhu
Children's Research Institute
Departments of Pediatrics and Internal Medicine
The University of Texas Southwestern Medical Center
Dallas, TX 75390, USA
The ORCID identification number(s) for the author(s) of this article can be found under https://doi.org/10.1002/adma.201805308.

DOI: 10.1002/adma.201805308

Table 1. Details of Library A and Library B DLNP formulations, including determinate molar ratio and percentage of each component, and the weight ratio of 5A2-SC8 to mRNA. See Table S1 (Supporting Information) for physical characterization of DLNP diameter and surface charge.

	Library A								
	Molar Ratios				Molar Percentage [%]				
Name	5A2-SC8	DOPE	Chol	DMG-PEG	5A2-SC8	DOPE	Chol	DMG-PEG	5A2-SC8/mRNA (wt/wt)
A1	15	10	20	0.5	32.97	21.98	43.96	1.10	20
A2	15	20	25	1	24.59	32.79	40.98	1.64	20
A3	15	30	30	2.5	19.35	38.71	38.71	3.23	20
A4	15	40	35	5	15.79	42.11	36.84	5.26	20
A5	25	10	25	2.5	40.00	16.00	40.00	4.00	20
A6	25	20	20	5	35.71	28.57	28.57	7.14	20
A7	25	30	35	0.5	27.62	33.15	38.67	0.55	20
A8	25	40	30	1	26.04	41.67	31.25	1.04	20
A9	35	10	30	5	43.75	12.50	37.50	6.25	20
A10	35	20	35	2.5	37.84	21.62	37.84	2.70	20
A11	35	30	20	1	40.70	34.88	23.26	1.16	20
A12	35	40	25	0.5	34.83	39.80	24.88	0.50	20
A13	45	10	35	1	49.45	10.99	38.46	1.10	20
A14	45	20	30	0.5	47.12	20.94	31.41	0.52	20
A15	45	30	25	5	42.86	28.57	23.81	4.76	20
A16	45	40	20	2.5	41.86	37.21	18.60	2.33	20
	Library B								
B1	5	10	15	0	16.67	33.33	50.00	0.00	20
B2	5	15	20	0.5	12.35	37.04	49.38	1.23	20
B3	5	20	25	1	9.80	39.22	49.02	1.96	20
B4	5	25	30	2	8.06	40.32	48.39	3.23	20
B5	10	10	20	1	24.39	24.39	48.78	2.44	20
B6	10	15	15	2	23.81	35.71	35.71	4.76	20
B7	10	20	30	0	16.67	33.33	50.00	0.00	20
B8	10	25	25	0.5	16.53	41.32	41.32	0.83	20
B9	15	10	25	2	28.85	19.23	48.08	3.85	20
B10	15	15	30	1	24.59	24.59	49.18	1.64	20
B11	15	20	15	0.5	29.70	39.60	29.70	0.99	20
B12	15	25	20	0	25.00	41.67	33.33	0.00	20
B13	20	10	30	0.5	33.06	16.53	49.59	0.83	20
B14	20	15	25	0	33.33	25.00	41.67	0.00	20
B15	20	20	20	2	32.26	32.26	32.26	3.23	20
B16	20	25	15	1	32.79	40.98	24.59	1.64	20

As a core component of this effort to overcome the issue of exaggerated carrier toxicity in diseases with high liver dysfunction, we recently reported a large library of >1500 ester-based dendrimers containing ionizable amino groups that self-assemble with excipients into dendrimer-based lipid nanoparticles (DLNPs) to effectively deliver siRNAs/miRNAs to compromised livers.[6] A dendrimer named 5A2-SC8 emerged from this screen and was further validated for therapeutic use in aggressive and challenging genetically engineered mouse models of *MYC*-driven liver cancer[6,7] and for toggling the polyploid state in the liver via delivery of small 18–22 base pair siRNAs/miRNAs.[8] However, we found that 5A2-SC8 DLNP compositions optimized for small RNAs (cationic ionizable lipid/phospholipid/cholesterol/lipid poly(ethylene glycol) (PEG) = 50/10/38/2 (mol/mol)) were minimally effective for delivering long RNAs (e.g., ≈1300 nucleotide FAH mRNA). More broadly, LNPs have been widely employed to deliver siRNAs/miRNAs to the liver, including in human clinical trials,[9] but it remains challenging to rationally redesign LNPs for delivery of much longer cargo such as mRNA.[2,3,10]

In this work, we undertook systematic optimization of DLNPs to yield a highly tolerable carrier for efficacious delivery

of FAH mRNA that produces functional FAH protein, restores normal enzyme function in the liver, stabilizes normal body weight, and extends survival in FAH$^{-/-}$ knockout (KO) mice (Figure S1, Supporting Information; Figure 6). We found that optimal mRNA formulations require significantly decreasing the molar amount of ionizable cationic lipid, increasing the molar amount of zwitterionic phospholipid, and slightly increasing cholesterol and lipid poly(ethylene glycol) to render LNPs with high loading of mRNA and a charge balance that facilitates mRNA release. Optimized mRNA DLNPs (mDLNPs) transfected >44% of all hepatocytes the liver, yielded high FAH protein levels at low mRNA doses, and were well tolerated in an HT-1 mouse model with compromised liver function. Control FAH$^{-/-}$ mice died within three weeks after induction of hepatorenal tyrosinemia. Remarkably, survival of FAH$^{-/-}$ mice treated with FAH mRNA mDLNPs was extended indefinitely without any signs of disease, weight loss, or liver complications. We believe this study provides a framework for the rational optimization of LNPs to improve LNP delivery of mRNA broadly and introduces a specific and viable DLNP carrier with translational potential to treat genetic diseases of the liver.

It has emerged over the past few years that carriers for delivery of small 18–22 base pair siRNAs/miRNAs often require optimization to be able to package and release longer mRNAs effectively. Recent efforts that applied orthogonal experimental design methodologies to empirically optimize lipid and lipid-like nanoparticles for mRNA delivery have highlighted that adjustment of individual LNP components can improve mRNA delivery efficacy.[10d,e] We and others have hypothesized that internal RNA solubilizing and stabilizing interactions improve LNP organization and increase delivery efficacy.[10d,e,g–i,n,11] For example, we showed that hybrid zwitterionic amino lipids (ZALs) can self-assemble into LNPs without phospholipid to load, stabilize, and release mRNAs intracellularly.[11c] Further investigating the fundamental role of each LNP component in a classic 4-component LNP, we realized that phospholipids mediate RNA loading into LNPs. Studies involving titration of phospholipid into cationic lipid formulations clearly showed that phospholipid was not necessary for siRNA delivery but was required for mRNA delivery.[11c] Increasing phospholipid content progressively improved mRNA loading into the LNP and promoted delivery. This prior work has supported our hypothesis that molecular interactions surrounding RNAs in water pockets within LNPs must be critically balanced to enable efficacy of longer RNAs. Because initial ZAL formulations delivered mRNA predominantly to the lungs and DLNPs delivered small RNAs to liver hepatocytes, we aimed herein to use the knowledge learned from these separate studies to rationally

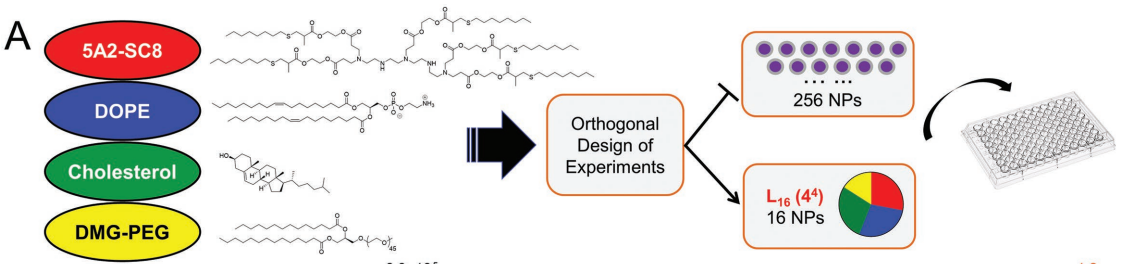

B

Level	Molar Ratios of DLNPs			
	5A2-SC8	DOPE	Chol	DMG-PEG
1	15	10	2	0.5
2	25	20	25	1
3	35	30	30	2.5
4	45	40	35	5

Library A: $L_{16}(4^4)$ = 16 NPs

C

Level	Molar Ratios of DLNPs			
	5A2-SC8	DOPE	Chol	DMG-PEG
1	5	10	15	0
2	10	15	20	0.5
3	15	20	25	1
4	20	25	30	2

Library B: $L_{16}(4^4)$ = 16 NPs

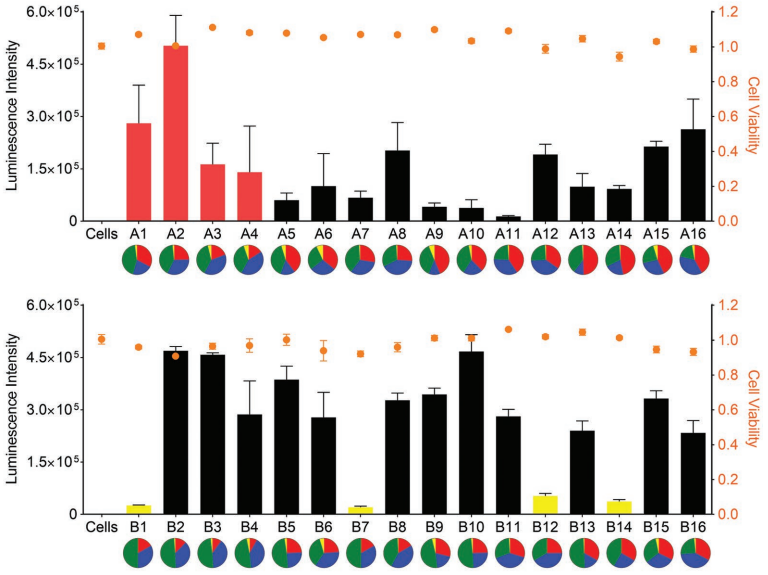

Figure 1. Systematic optimization of DLNPs improved delivery efficacy of mRNA. IGROV-1 cells were treated with various DLNP formulations containing Luciferase mRNA (25 ng mRNA per well; 96-well plate (n = 4)). Luminescence intensity and cell viability were quantified 24 h after transfection. A) Design of Experiment (DOE) calculations minimized the number of formulations needed to improve formulation molar ratios. An $L_{16}(4^4)$ orthogonal table design was employed to guide further optimization across two rounds of screening. B) Red bars highlight more effective DLNPs with a lower fraction of ionizable cationic lipid. C) Yellow bars highlight the loss of activity when no DMG-PEG was included. See Table 1 for molar ratios and molar percentages used in each of the 32 formulations.

Name	Molar Ratios of DLNPs				5A2-SC8/mRNA (wt/wt)	Note [a,b]
	5A2-SC8	DOPE	Chol	DMG-PEG		
C1	5	20	25	1	10	B3 (10/1, 1.96%)
C2	5	20	25	1	20	B3 (20/1, 1.96%)
C3	5	20	25	1	30	B3 (30/1, 1.96%)
C4	5	20	25	1.5	20	B3 (20/1, 2.91%)
C5	5	20	25	2.5	20	B3 (20/1, 4.76%)
C6	15	15	30	1	10	B10 (10/1, 1.64%)
C7	15	15	30	1	20	B10 (20/1, 1.64%)
C8	15	15	30	1	30	B10 (30/1, 1.64%)
C9	15	15	30	2	20	B10 (20/1, 3.23%)
C10	15	15	30	3	20	B10 (20/1, 4.76%)
C11	15	15	20	1	20	BX1 (20/1, 1.96%)
C12	5	15	20	1	20	BX2 (20/1, 2.44%)

[a] The number before the comma represents weight ratio of 5A2-SC8 to mRNA, and the number after the comma represents molar percent of DMG-PEG;

[b] Both BX1 and BX2 represent the suggested molar ratios from software.

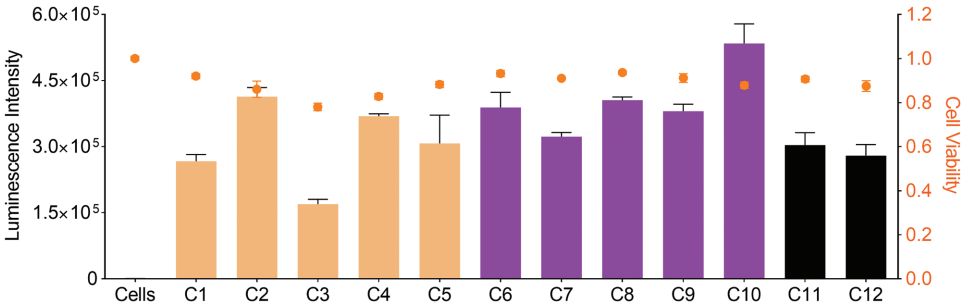

Figure 2. Optimization of DMG-PEG content and carrier to mRNA weight ratio further improved efficacy. The effects of DMG-PEG percent and weight ratios for mRNA delivery potency were evaluated. We selected top two formulations (B3 and B10) from Library B and systematically adjusted the DMG-PEG percentage from 1.96% to 4.76%, and the weight ratio of 5A2-SC8 to mRNA from 10/1 to 30/1 to examine the effects on Luc mRNA delivery (25 ng mRNA per well; 96-well plate ($n = 4$)). Luminescence intensity and cell viability were quantified 24 h after transfection.

redesign DLNP carriers for improved mRNA delivery to the liver for HT-1 treatment. Moreover, because it is not always clear if existing data will hold for other carriers, we decided to evaluate if optimization of DLNPs could lead to more effective mRNA carriers that could function in an HT-1 mouse model with compromised liver function.

The relative molar ratios of lipids within DLNPs were initially adjusted in the following relative ranges: 5A2-SC8 (15 to 45), 1,2-dioleoyl-sn-glycero-3-phosphoethanolamine (DOPE) (10 to 40), cholesterol (20 to 35), and DMG-PEG2000 (0.5 to 5.0) (**Table 1**). Luciferase (Luc) mRNA was used as a reporter sequence to evaluate delivery to IGROV-1 ovarian cancer cells in vitro as a representative line with moderate resistance to transfection (**Figure 1**). Right away, we noted that formulations A1–A4 were equal to or more effective than A5–A16. Surprisingly, A1–A4 contain the lowest relative proportion of ionizable cationic 5A2-SC8 (15) (Table 1). Comparing to standard siRNA formulations that frequently require 50 mole % of the LNP to be composed of the cationic lipid, we found that the cationic lipid can be dramatically decreased in effective mRNA formulations. Moreover, relative increases of zwitterionic DOPE were also advantageous for efficacy (A4, A8, A12, A16). Given that long mRNAs are flexible and present thousands of anionic phosphates per molecule with which to interact with protonated 5A2-SC8 amines at the low pH of mixing, this suggests that these electrostatic interactions cannot be too strong; that instead, a balance of cationic lipids and zwitterionic phospholipids is ideal for association with mRNA solvated with water molecules and salt ions.[12] In contrast, short siRNAs (only 18–22 base pairs) may resemble rigid rods, where molecular interactions involve hydrophobic forces in addition to weaker electrostatic interactions compared to mRNAs. Thus, initial results from the DLNP optimization revealed that mRNAs may require weaker electrostatic associations, likely to allow for mRNA release after endocytosis. Plotting of this data set as a function of each component revealed a trend for lower ionizable cationic lipid and higher phospholipid (Figure S2A, Supporting Information) to maximize activity. No decrease in cellular viability was observed, which was attributed to the low toxicity of the ester-based degradable 5A2-SC8.

We next focused the B round of optimization on proportionally lower 5A2-SC8 (5 to 20) and DOPE (10 to 25) ratios, with higher relative cholesterol (15 to 30) fractions (Figure 1C). We also examined the role of 1,2-dimyristoyl-sn-glycerol-methoxy poly(ethylene glycol) 2000 (DMG-PEG). This second round of screening revealed more hits overall (Figure S2B, Supporting Information), suggesting that the adjustments predicted from

Library A were favorable. Notably, DLNPs prepared without DMG-PEG (B1, B7, B12, B14) exhibited very low mRNA delivery capability which may be due to DLNP aggregation (Table S1, Supporting Information). These results indicate that DMG-PEG is essential for DLNP stability.

Following establishment of optimized formulations that contained significantly decreased 5A2-SC8 and increased DOPE, we created a third round of DLNPs that focused on lead DLNPs B3 and B10 and studied the effects of PEGylation and carrier:mRNA weight ratio (**Figure 2**). Interestingly, weight ratios of 5A2-SC8:mRNA did not exhibit significant influence for mRNA delivery, which is in contrast to trends well established for siRNA delivery.[6] Compared with siRNA formulations, we found that mRNA formulations could tolerate higher proportions of DMG-PEG, with the highest efficacy reached at 4.76% (C10). We also tested C11, C12 which were optimal ratios predicted by software. Interestingly, these new DLNPs were less active than the best DLNPs from Library C, suggesting that each of the 5 components in an LNP is not an independent variable. Instead, there is interplay between these factors to construct optimally arranged DLNPs that ultimately achieve effective mRNA delivery. To examine the mechanism of high mRNA delivery potency, confocal imaging was conducted with B7 (low activity), A3 (medium activity), and C10 (high activity) formulations. As shown in Figure S3 (Supporting Information), stronger intracellular Cy5-labeled mRNA fluorescence was observed for A3 and C10 DLNPs than for B7 at 2 and 8 h following treatment. Furthermore, B7 DLNPs were visualized in punctate spots (white arrows), while images of A3 and C10 DLNPs showed diffused fluorescence (yellow arrows), which has previously been ascribed to indicate better endosomal escape.[13] These results demonstrated that higher mRNA delivery efficacy of DLNPs involved enhancement of cellular uptake and endosomal escape.

We next examined the ability of the top formulations from all three libraries to deliver Luc mRNA in vivo. All four DLNPs were able to productively deliver Luc mRNA to the liver following intravenous (IV) administration (**Figure 3**, Figure S4, Supporting Information). Among these, C10 enabled the highest Luc expression in the liver at the tested dose of 0.25 mg kg^{-1}. Interestingly, the C4 DLNPs were noticeably less efficacious than the others. The major difference is that C4 has > twofold less ionizable 5A2-SC8 lipid (9.71 mole %) than the other formulations (≈23 mole%). These results indicated that while

A

Name	Molar Ratios				Molar Percentage (%)				5A2-SC8/mRNA (wt/wt)
	5A2-SC8	DOPE	Chol	DMG-PEG	5A2-SC8	DOPE	Chol	DMG-PEG	
A2 (20/1, 4.76%)	15	20	25	3	23.81	31.75	39.68	4.76	20
C4 (20/1, 2.91%)	5	20	25	1.5	9.71	38.83	48.54	2.91	20
C9 (20/1, 3.23%)	15	15	30	2	24.19	24.19	48.39	3.23	20
C10 (20/1, 4.76%)	15	15	30	3	23.81	23.81	47.62	4.76	20

B

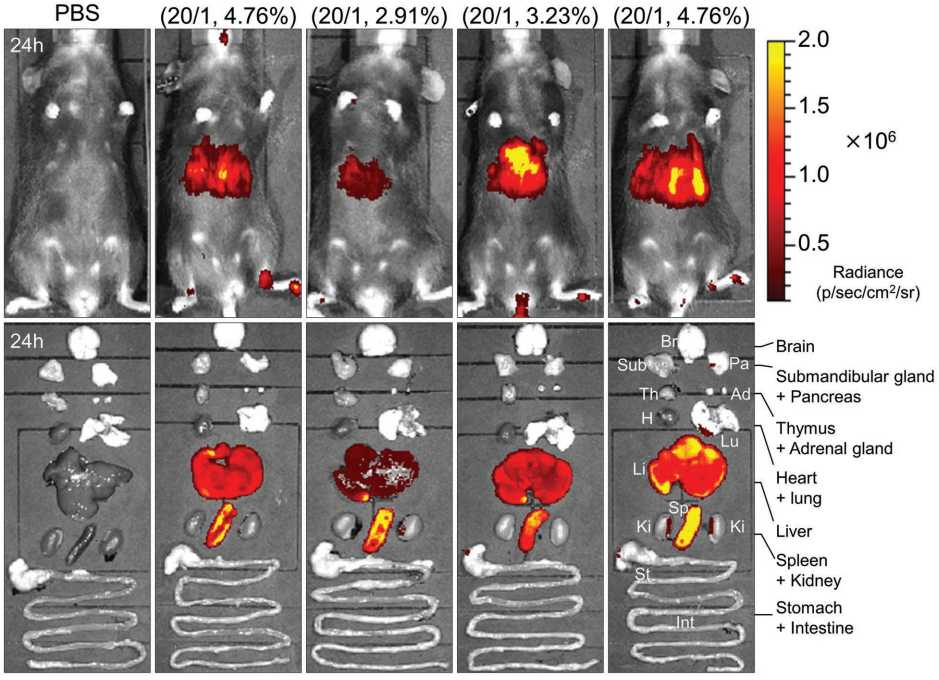

Figure 3. In vivo screening of Luc mRNA delivery further evaluated the DLNP optimization process. Top formulations (A2, C4, C9 and C10) were examined for their ability to deliver Luc mRNA in vivo. A) Formulation details. B) C57BL/6 mice were randomly grouped and injected IV with 0.25 mg kg^{-1} Luc mRNA (n = 2). Luminescence was quantified 24 h after injection.

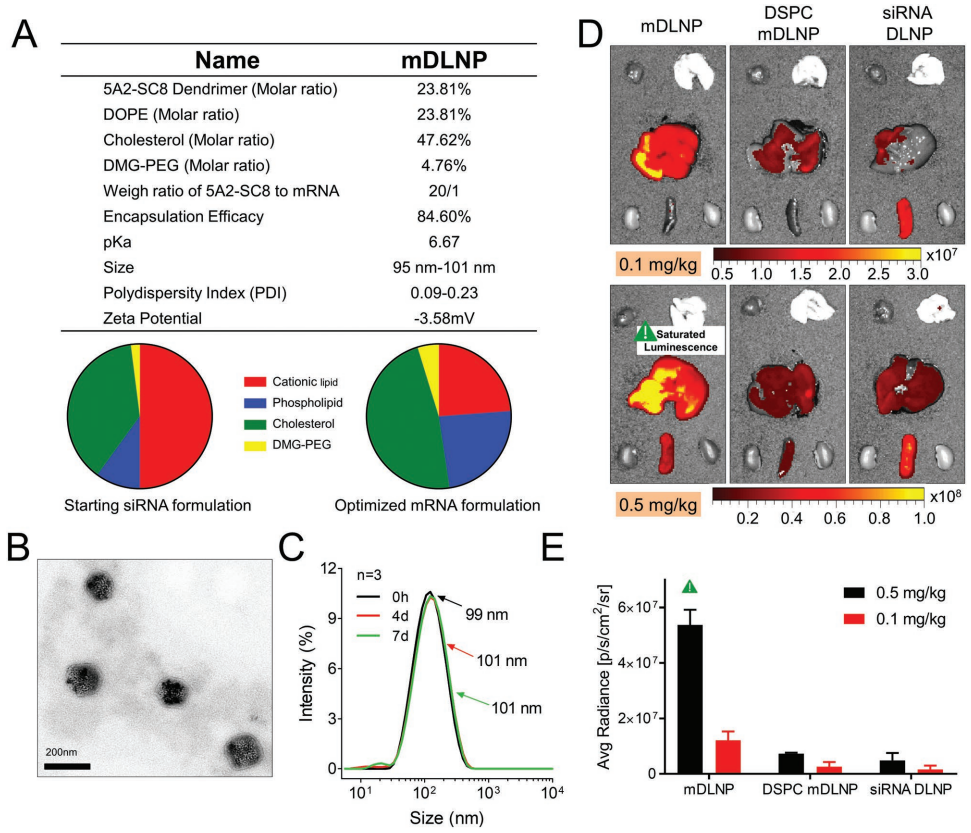

Figure 4. Characterization of the optimized mDLNP formulation revealed physical attributes amendable to clinical translation. Standard siRNA formulations were significantly less efficacious in vivo for delivery of mRNA than optimized mDLNP formulations. A) Table showing the detailed molar ratios between each component, weight ratio of 5A2-SC8 to mRNA, encapsulation efficiency, pKa, size, and zeta-potential. B) The morphology of mDLNPs is shown in the TEM image (scale bar = 200 nm). C) DLNP stability was monitored by DLS ($n = 3$) for one week. D,E) mDLNPs containing DOPE were more efficacious than mDLNPs containing DSPC and the starting siRNA DLNPs. Ex vivo bioluminescence images following at 0.1 and 0.5 mg kg^{-1} (I.V.) are shown ($n = 2$). The green triangle denotes detector saturation. The average luminescence for the whole livers was plotted (E).

5A2-SC8 could be decreased by more than half compared to the fraction in a typical siRNA formulation, it is required for delivery (see Figures 2 and 3). From this result, we selected the C10 formulation as the optimal composition for liver delivery of mRNA. Given the large differences from the starting siRNA formulation, we hereafter designate C10 as a messenger RNA optimized DLNP (mDLNP).

We then performed physical characterization (**Figure 4**). mDLNPs were monodisperse with a diameter around 100 nm and a near neutral surface charge (–3.58 mV) due to the high amount (4.76%) of DMG-PEG shielding. mDLNPs showed a clear improvement in comparison to initial formulations (Figure S5, Supporting Information). mDLNPs were stable (no change in diameter) over the course of one week of monitoring in PBS at both 4 and 37 °C (Figure 4C, Figure S6, Supporting Information) and for two days under challenging 10% FBS media conditions at 37 °C (Figure S6, Supporting Information). Overall, we note four conclusions regarding the optimization study comparing an mRNA formulation to a siRNA formulation: 1. The mole fraction of ionizable cationic lipid should be decreased dramatically but not to zero (required for mRNA release); 2. The mole fraction of zwitterionic phospholipid should be increased greatly (aids mRNA loading into DLNPs and augments release); 3. Cholesterol is important for DLNP stability above the ionizable lipid pKa (moderate mole fraction is ideal, efficacy is less sensitive changing cholesterol); 4. Lipid PEG is required for DLNP stability (mRNA DLNPs can tolerate higher DMG-PEG mole fractions). Notably, mDLNPs containing DOPE were more efficacious than mDLNPs containing DSPC and the starting siRNA DLNPs (Figure 4D,E and Figure S7, Supporting Information). These general design guidelines can likely be applied to other cationic ionizable lipid-based 4 component LNPs[3] to improve mRNA delivery efficacy.

To further understand mDLNP delivery to the liver, we quantified time dependent Luc activity following IV administration. Luc protein expression peaked at 6 h post-injection and persisted for about two days at a high level (10^7 photons s^{-1}, 0.25 mg kg^{-1}) at the organ (**Figure 5**A) and whole-body level (Figure S8, Supporting Information). We next examined the in vivo dose responsive behavior of delivery (Figure 5B). Luc expression increased with increasing dose from 0.05 mg kg^{-1} to 0.2 mg kg^{-1} mRNA. Average radiance across the whole livers was calculated and plotted for both the time-dependent and dose response studies (Figure 5A,B). With expression above 10^6 photons s^{-1} at a 0.05 mg kg^{-1} mRNA dose, mDLNPs are likely the most efficacious mRNA carrier reported to date. Next, we quantified delivery to liver hepatocytes. We delivered mCherry mRNA at a dose of 0.5 mg kg^{-1} and compared mCherry

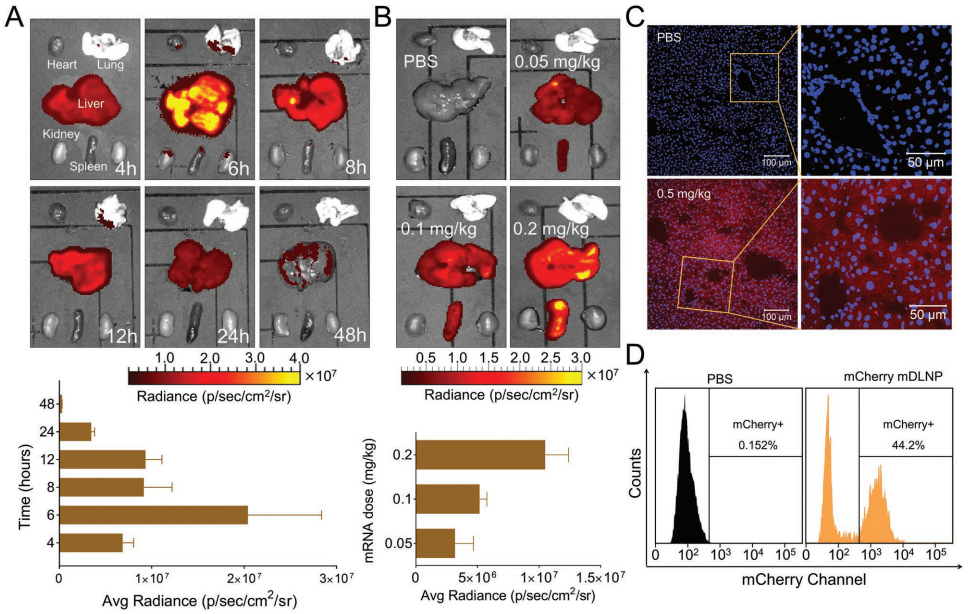

Figure 5. mDLNPs deliver mRNA in a dose-dependent manner with high transfection efficiency of liver hepatocytes. A) Time-dependent Luc expression in C57BL/6 mice following IV injection of 0.25 mg kg^{-1} Luc mRNA in mDLNPs. Luminescence was recorded at various time-points within 48h ($n = 2$). B) For dose-dependent Luc mRNA expression, C57BL/6 mice were injected IV with the doses of 0.05, 0.1, or 0.2 mg kg^{-1}. Luminescence was detected 6h post injection ($n = 2$). C) Confocal images of mCherry expression in liver cryo-sections following IV injection of 0.5 mg kg^{-1} mCherry mRNA (6 h, nuclei are blue, mCherry protein is red, scale bar = 50 µm). D) In vivo transfection efficacy of hepatocytes detected by flow cytometry. C57BL/6 mice were injected with mCherry mDLNPs at a dose of 0.5 mg kg^{-1}. Primary hepatocytes were isolated after 6h and analyzed by flow cytometry.

expression to PBS injected controls by fluorescence imaging of liver sections (Figure 5C). Strong red mCherry signal was observed throughput the liver (Figure S9, Supporting Information). To further analyze transfection efficiency, we isolated hepatocytes from injected mice and used flow cytometry to quantify mCherry mRNA delivery specifically to hepatocytes. We found that 44.2% of all hepatocytes were strongly expressing mCherry protein 6 h following IV administration of mCherry mRNA mDLNPs. We note that mutations in FAH have been corrected using CRISPR/Cas components delivered by hydrodynamic injection[14] or by combining non-viral delivery of Cas9 mRNA with viral delivery of sgRNA and DNA.[15] Currently, the efficiency of these processes has been very low, reported as 0.4% and 6% of hepatocytes in prior publications.[14a,15] We therefore believe that protein replacement of FAH via mRNA using optimized mDLNPs is a viable approach due to the high fraction of hepatocytes that express functional protein (>44%). Using multiple rounds of an in vitro/in vivo orthogonal experimental design methodology, we arrived at a formulation with potential to deliver enough FAH mRNA (Figure S10, Supporting Information) to have a therapeutic benefit in diseased mice.

To evaluate efficacy for FAH protein replacement therapy, we employed a knockout model of HT-1 disease (FAH$^{-/-}$), which was created by insertion of 1819 nucleotides into exon 5 of the FAH gene. Therefore, this mouse model is optimal for evaluating protein replacement therapy via mRNA delivery, and less suitable for correction by gene editing. First, we evaluated the ability of mDLNPs to deliver FAH mRNA by measuring FAH protein expression in the liver using immunofluorescence staining (**Figure 6**B). Strong FAH antibody staining was observed throughout the liver sections.

FAH$^{-/-}$ mice are typically maintained on NTBC to reduce symptoms of HT-1. Once off NTBC, FAH$^{-/-}$ mice immediately start to lose body weight, build up toxic levels of metabolites including succinylacetone, and succumb to death from liver failure. To examine the therapeutic efficacy of FAH mRNA therapy, we removed FAH$^{-/-}$ mice from NTBC water and subsequently treated them with IV injections of 10 µg FAH mRNA per mouse every 3 days in mDLNPs (about 0.35 mg kg^{-1}) (Figure 6A). This dose and schedule were selected based mRNA delivery kinetics. The body weight of the mice was monitored for 30 days. PBS injections and mCherry mDLNPs served as controls. FAH$^{-/-}$ mice injected with PBS or mCherry mRNA control mDLNPs lost more than 20% of their body mass within three weeks. In contrast, FAH$^{-/-}$ mice treated with FAH mRNA mDLNPs were active, healthy, and did not lose any weight (Figure 6C). Survival was extended with continued mRNA treatment. Although the experiment was halted after one month, continuous mRNA delivery would likely mediate survival indefinitely.

To confirm that FAH protein production was the cause of increased survival, we detected FAH by western blot of isolated livers (Figure 6D). Strong FAH protein expression was observed only in the FAH mRNA treated mice. In addition, FAH$^{-/-}$ mice treated with FAH mRNA mDLNPs had equivalent levels of TBIL, ALT, and AST compared to wild type C57BL/6 mice and FAH$^{-/-}$ mice maintained on NTBC (Figure 6E). In contrast, FAH$^{-/-}$ mice injected with PBS or mCherry control mDLNPs had elevated liver damage markers. This challenging experiment, performed in FAH$^{-/-}$ mice that harbor compromised livers, demonstrates that 5A2-SC8 mDLNPs have the ability to productively deliver FAH mRNA to hepatocytes to produce

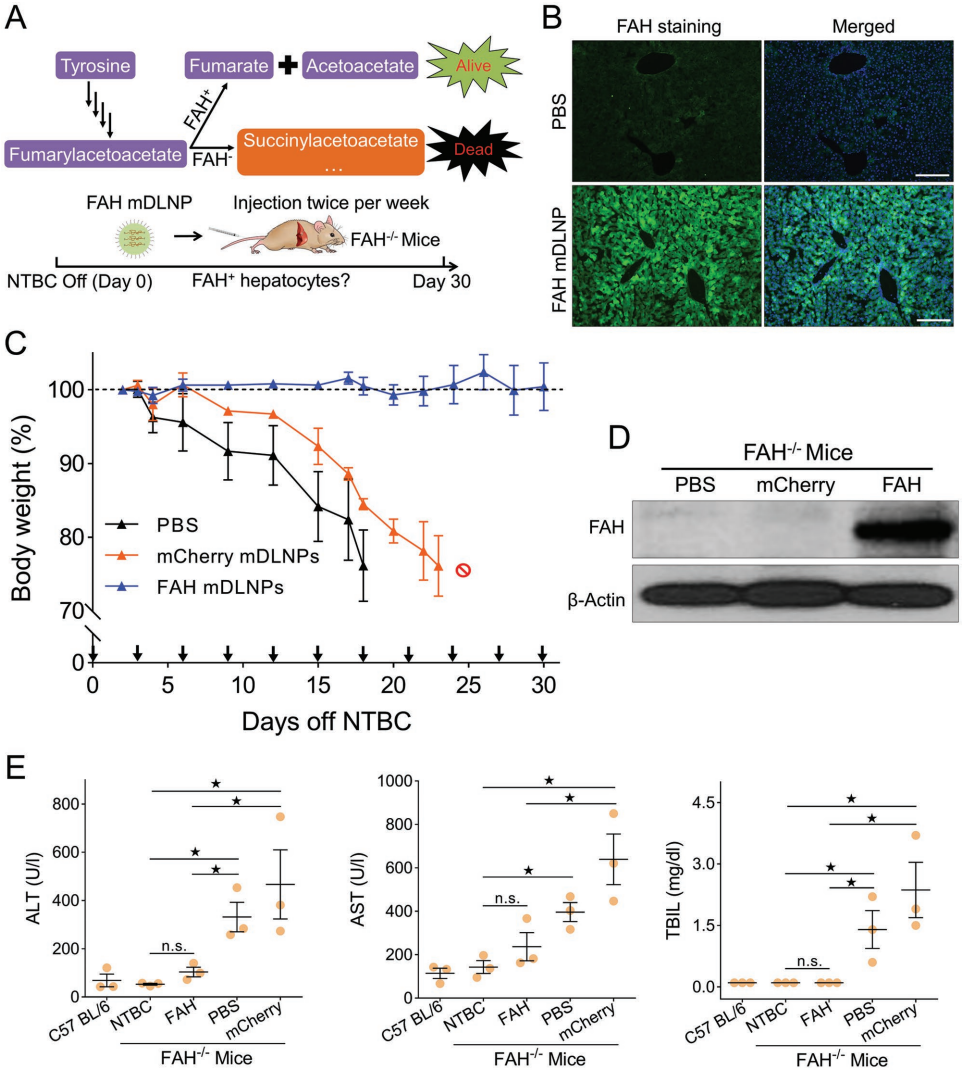

Figure 6. mDLNP delivery of FAH mRNA normalized body weight and liver function in FAH$^{-/-}$ mice. A) Scheme of therapeutic regimen. B) Immunofluorescence (IF) images of liver sections following injection of FAH mRNA in mDLNPs (10 µg mRNA per mouse, 6h, scale bar = 250 µm). C) Body weights of FAH$^{-/-}$ mice were monitored in a one month therapy study. Mice (off NTBC water, 2♂, 1♀, $n = 3$) were randomly grouped and injected with PBS, mCherry mDLNPs, or FAH mDLNP every three days (denoted by arrows) until day 30 (10 µg mRNA per injection, about 0.35 mg kg^{-1}). The red crossed circle denotes euthanasia due to IACUC animal welfare requirements. At the end point for each mouse, D) western blot of liver tissue and E) liver damage markers (TBIL, ALT and AST) were measured to evaluate the therapeutic effects. Not significant: $P > 0.05$.* denotes $P < 0.05$.

therapeutically efficacious levels of FAH protein over an extended period of time. This delivery system therefore has the capability to function in a compromised host with liver disease. The ability to deliver high levels of FAH mRNA to > 40% of all hepatocytes to normalize body weight and liver function demonstrates the utility of 5A2-SC8 mDLNPs for treatment of HT-1.

To improve therapeutic delivery of FAH mRNA to the liver, we reasoned that efficacious carriers would have to be highly tolerated in the livers of mice with compromised liver function, as well as be fundamentally altered in their molar composition to accommodate high loading of long mRNAs with potential for secondary folding and increased electrostatic binding. Despite the empirical evidence that reformulation can increase the ability of LNPs to deliver mRNA, a framework for the rational design of LNPs for long RNAs remains unclear, particularly regarding the roles that each lipid play. To answer these questions and to develop LNPs that can mediate high mRNA delivery for functional protein replacement of FAH, we employed a systematic orthogonal matrix design methodology designed to elucidate functional contributions of each lipid within LNPs for efficacious mRNA delivery. We selected 5A2-SC8 as the ionizable cationic dendrimer because it has been successful for siRNA delivery to the liver for investigating gene functionality in cancer development and liver regeneration without concern for material toxicity-induced off-target effects.[6,7b,8] Ionizable cationic lipids are essential for RNA delivery because they bind RNAs at low pH during mixing, and promote intracellular release as the pH decreases during endosomal maturation.[11d,16] DOPE was used as the phospholipid due to its productive utility in mRNA formul ations.[10d,g–i,11a,c] DOPE enhances RNA loading[11c] and may form unstable hexagonal phases to aid LNP disassembly and

endosome membrane destabilization.[10m,12,17] Inspired by previous reports that optimized lipidoid and lipid-like nanoparticles for mRNA delivery, we examined whether orthogonal experimental design methodologies could be applied to optimize 5A2-SC8 dendrimer lipid DLNPs.[10d,e] Without knowing a priori how each component of the LNP should be adjusted, we used multiple rounds of optimization involving testing 44 DLNPs that cover the theoretical space of >500 formulations. This is important, given that LNPs require a balance of molecular interactions to stabilize long mRNAs where individual parameters may counteract each other. These rounds of Library screening (A, B, and C) sequentially improved mRNA delivery.

Ultimately, this process of systematic optimization allowed development of a non-toxic degradable delivery system that enhanced delivery of full length mRNAs to liver hepatocytes. Due to the high in vivo transfection efficiency and efficacy, 5A2-SC8 mDLNPs were able to extend survival in $FAH^{-/-}$ knockout mice suffering from HT-1. FAH mRNA treatment normalized body mass and liver function through the entire 30 d experiment. In the course of this work, we found that LNPs optimized for mRNA delivery should contain significantly less ionizable cationic lipid and more zwitterionic phospholipids compared to standard siRNA formulations. This provides a rational design guideline to redevelop other siRNA-delivering LNPs for delivery of mRNA. Moreover, the capability of 5A2-SC8 mDLNPs to deliver FAH mRNA to diseased livers without any carrier toxicity makes this system suitable for treatment of a wide variety of liver diseases.

Supporting Information

Supporting Information is available from the Wiley Online Library or from the author.

Acknowledgements

D.J.S. acknowledges financial support from the Department of Defense (CA150245P3), American Cancer Society (RSG-17-012-01), Cancer Prevention and Research Institute of Texas (CPRIT) (R1212), and Welch Foundation (I-1855). H.Z. was supported by an NIH/NCI R01 grant (R01CA190525), a Burroughs Welcome Career Award for Medical Scientists, and a CPRIT Individual Investigator Award (RP180268). All animal experiments in this study were approved by the Institution Animal Care and Use Committees of The University of Texas Southwestern Medical Center and were consistent with local, state, and federal regulations as applicable.

Conflict of Interest

D.J.S. is a co-founder of, and consultant to, ReCode Therapeutics.

Keywords

gene therapy, lipid nanoparticles (LNPs), mRNA delivery, nanoparticle formulations, protein replacement therapy

Received: August 14, 2018
Revised: September 14, 2018
Published online: October 25, 2018

[1] J. M. Chinsky, R. Singh, C. Ficicioglu, C. D. M. van Karnebeek, M. Grompe, G. Mitchell, S. E. Waisbren, M. Gucsavas-Calikoglu, M. P. Wasserstein, K. Coakley, C. R. Scott, *Genet. Med.* **2017**, *19*.

[2] U. Sahin, K. Kariko, O. Tureci, *Nat. Rev. Drug Discovery* **2014**, *13*, 759.

[3] K. A. Hajj, K. A. Whitehead, *Nat. Rev. Mater.* **2017**, *2*, 17056.

[4] a) R. J. Chandler, M. C. LaFave, G. K. Varshney, N. S. Trivedi, N. Carrillo-Carrasco, J. S. Senac, W. Wu, V. Hoffmann, A. G. Elkahloun, S. M. Burgess, C. P. Venditti, *J. Clin. Invest.* **2015**, *125*, 870; b) R. J. Chandler, M. S. Sands, C. P. Venditti, *Hum. Gene Ther.* **2017**, *28*, 314.

[5] a) S. Y. Wu, G. Lopez-Berestein, G. A. Calin, A. K. Sood, *Sci. Transl. Med.* **2014**, *6*, 240; b) J. D. Tousignant, A. L. Gates, L. A. Ingram, C. L. Johnson, J. B. Nietupski, S. H. Cheng, S. J. Eastman, R. K. Scheule, *Hum. Gene Ther.* **2000**, *11*, 2493; c) H. T. Lv, S. B. Zhang, B. Wang, S. H. Cui, J. Yan, *J. Controlled Release* **2006**, *114*, 100.

[6] K. Zhou, L. H. Nguyen, J. B. Miller, Y. Yan, P. Kos, H. Xiong, L. Li, J. Hao, J. T. Minnig, H. Zhu, D. J. Siegwart, *Proc. Natl. Acad. Sci. USA* **2016**, *113*, 520.

[7] a) L. Wu, L. H. Nguyen, K. Zhou, T. Y. de Soysa, L. Li, J. B. Miller, J. Tian, J. Locker, S. Zhang, G. Shinoda, M. T. Seligson, L. R. Zeitels, A. Acharya, S. C. Wang, J. T. Mendell, X. He, J. Nishino, S. J. Morrison, D. J. Siegwart, G. Q. Daley, N. Shyh-Chang, H. Zhu, *eLife* **2015**, *4*, e09431; b) S. Zhang, L. H. Nguyen, K. Zhou, H. C. Tu, A. Sehgal, I. Nassour, L. Li, P. Gopal, J. Goodman, A. G. Singal, A. Yopp, Y. Zhang, D. J. Siegwart, H. Zhu, *Gastroenterology* **2018**, *154*, 1421.

[8] S. Zhang, K. Zhou, X. Luo, L. Li, H. C. Tu, A. Sehgal, L. H. Nguyen, Y. Zhang, P. Gopal, B. D. Tarlow, D. J. Siegwart, H. Zhu, *Dev. Cell* **2018**, *44*, 447.

[9] a) R. Kanasty, J. R. Dorkin, A. Vegas, D. Anderson, *Nat. Mater.* **2013**, *12*, 967; b) T. Coelho, D. Adams, A. Silva, P. Lozeron, P. N. Hawkins, T. Mant, J. Perez, J. Chiesa, S. Warrington, E. Tranter, M. Munisamy, R. Falzone, J. Harrop, J. Cehelsky, B. R. Bettencourt, M. Geissler, J. S. Butler, A. Sehgal, R. E. Meyers, Q. M. Chen, T. Borland, R. M. Hutabarat, V. A. Clausen, R. Alvarez, K. Fitzgerald, C. Gamba-Vitalo, S. V. Nochur, A. K. Vaishnaw, D. W. Y. Sah, J. A. Gollob, O. B. Suhr, *N. Engl. J. Med.* **2013**, *369*, 819; c) D. Adams, O. B. Suhr, P. J. Dyck, W. J. Litchy, R. G. Leahy, J. Chen, J. Gollob, T. Coelho, *BMC Neurol.* **2017**, *17*, 181.

[10] a) M. S. Kormann, G. Hasenpusch, M. K. Aneja, G. Nica, A. W. Flemmer, S. Herber-Jonat, M. Huppmann, L. E. Mays, M. Illenyi, A. Schams, M. Griese, I. Bittmann, R. Handgretinger, D. Hartl, J. Rosenecker, C. Rudolph, *Nat. Biotechnol.* **2011**, *29*, 154; b) B. Petsch, M. Schnee, A. B. Vogel, E. Lange, B. Hoffmann, D. Voss, T. Schlake, A. Thess, K. J. Kallen, L. Stitz, T. Kramps, *Nat. Biotechnol.* **2012**, *30*, 1210; c) H. Uchida, K. Itaka, T. Nomoto, T. Ishii, T. Suma, M. Ikegami, K. Miyata, M. Oba, N. Nishiyama, K. Kataoka, *J. Am. Chem. Soc.* **2014**, *136*, 12396; d) K. J. Kauffman, J. R. Dorkin, J. H. Yang, M. W. Heartlein, F. DeRosa, F. F. Mir, O. S. Fenton, D. G. Anderson, *Nano Lett.* **2015**, *15*, 7300; e) B. Li, X. Luo, B. Deng, J. Wang, D. W. McComb, Y. Shi, K. M. Gaensler, X. Tan, A. L. Dunn, B. A. Kerlin, Y. Dong, *Nano Lett.* **2015**, *15*, 8099; f) N. Pardi, S. Tuyishime, H. Muramatsu, K. Kariko, B. L. Mui, Y. K. Tam, T. D. Madden, M. J. Hope, D. Weissman, *J. Controlled Release* **2015**, *217*, 345; g) O. S. Fenton, K. J. Kauffman, R. L. McClellan, E. A. Appel, J. R. Dorkin, M. W. Tibbitt, M. W. Heartlein, F. DeRosa, R. Langer, D. G. Anderson, *Adv. Mater.* **2016**, *28*, 2939; h) A. Jarzebinska, T. Pasewald, J. Lambrecht, O. Mykhaylyk, L. Kummerling, P. Beck, G. Hasenpusch, C. Rudolph, C. Plank, C. Dohmen, *Angew. Chem., Int. Ed.* **2016**, *55*, 9591; i) J. C. Kaczmarek, A. K. Patel, K. J. Kauffman, O. S. Fenton, M. J. Webber, M. W. Heartlein, F. DeRosa, D. G. Anderson, *Angew. Chem., Int. Ed.* **2016**, *55*, 13808; j) F. DeRosa, B. Guild, S. Karve, L. Smith, K. Love, J. R. Dorkin, K. J. Kauffman, J. Zhang, B. Yahalom, D. G. Anderson, M. W. Heartlein, *Gene Ther.* **2016**, *23*, 699;

k) S. Ramaswamy, N. Tonnu, K. Tachikawa, P. Limphong, J. B. Vega, P. P. Karmali, P. Chivukula, I. M. Verma, *Proc. Natl. Acad. Sci. USA* **2017**, *114*, E1941; l) J. M. Richner, S. Himansu, K. A. Dowd, S. L. Butler, V. Salazar, J. M. Fox, J. G. Julander, W. W. Tang, S. Shresta, T. C. Pierson, G. Ciaramella, M. S. Diamond, *Cell* **2017**, *169*, 176; m) S. Patel, N. Ashwanikumar, E. Robinson, A. DuRoss, C. Sun, K. E. Murphy-Benenato, C. Mihai, O. Almarsson, G. Sahay, *Nano Lett.* **2017**, *17*, 5711; n) R. L. Ball, K. A. Hajj, J. Vizelman, P. Bajaj, K. A. Whitehead, *Nano Lett.* **2018**, *18*, 3814.

[11] a) Y. Dong, J. R. Dorkin, W. Wang, P. H. Chang, M. J. Webber, B. C. Tang, J. Yang, I. Abutbul-Ionita, D. Danino, F. DeRosa, M. Heartlein, R. Langer, D. G. Anderson, *Nano Lett.* **2016**, *16*, 842; b) B. Li, X. Luo, B. Deng, J. B. Giancola, D. W. McComb, T. D. Schmittgen, Y. Dong, *Sci. Rep.* **2016**, *6*, 22137; c) J. B. Miller, S. Zhang, P. Kos, H. Xiong, K. Zhou, S. S. Perelman, H. Zhu, D. J. Siegwart, *Angew. Chem., Int. Ed.* **2017**, *56*, 1059; d) Y. Yan, H. Xiong, X. Zhang, Q. Cheng, D. J. Siegwart, *Biomacromolecules* **2017**, *18*, 4307.

[12] A. K. K. Leung, I. M. Hafez, S. Baoukina, N. M. Belliveau, I. V. Zhigaltsev, E. Afshinmanesh, D. P. Tieleman, C. L. Hansen, M. J. Hope, P. R. Cullis, *J. Phys. Chem. C* **2012**, *116*, 22104.

[13] D. V. Morrissey, J. A. Lockridge, L. Shaw, K. Blanchard, K. Jensen, W. Breen, K. Hartsough, L. Machemer, S. Radka, V. Jadhav, N. Vaish, S. Zinnen, C. Vargeese, K. Bowman, C. S. Shaffer, L. B. Jeffs, A. Judge, I. MacLachlan, B. Polisky, *Nat. Biotechnol.* **2005**, *23*, 1002.

[14] a) H. Yin, W. Xue, S. Chen, R. L. Bogorad, E. Benedetti, M. Grompe, V. Koteliansky, P. A. Sharp, T. Jacks, D. G. Anderson, *Nat. Biotechnol.* **2014**, *32*, 551; b) F. P. Pankowicz, M. Barzi, X. Legras, L. Hubert, T. Mi, J. A. Tomolonis, M. Ravishankar, Q. Sun, D. Yang, M. Borowiak, P. Sumazin, S. H. Elsea, B. Bissig-Choisat, K. D. Bissig, *Nat. Commun.* **2016**, *7*, 12642.

[15] H. Yin, C.-Q. Song, J. R. Dorkin, L. J. Zhu, Y. Li, Q. Wu, A. Park, J. Yang, S. Suresh, A. Bizhanova, A. Gupta, M. F. Bolukbasi, S. Walsh, R. L. Bogorad, G. Gao, Z. Weng, Y. Dong, V. Koteliansky, S. A. Wolfe, R. Langer, W. Xue, D. G. Anderson, *Nat. Biotechnol.* **2016**, *34*, 328.

[16] a) O. Zelphati, F. C. Szoka Jr., *Proc. Natl. Acad. Sci. USA* **1996**, *93*, 11493; b) I. M. Hafez, N. Maurer, P. R. Cullis, *Gene Ther.* **2001**, *8*, 1188; c) G. Sahay, W. Querbes, C. Alabi, A. Eltoukhy, S. Sarkar, C. Zurenko, E. Karagiannis, K. Love, D. Chen, R. Zoncu, Y. Buganim, A. Schroeder, R. Langer, D. G. Anderson, *Nat. Biotechnol.* **2013**, *31*, 653; d) J. Gilleron, W. Querbes, A. Zeigerer, A. Borodovsky, G. Marsico, U. Schubert, K. Manygoats, S. Seifert, C. Andree, M. Stoter, H. Epstein-Barash, L. Zhang, V. Koteliansky, K. Fitzgerald, E. Fava, M. Bickle, Y. Kalaidzidis, A. Akinc, M. Maier, M. Zerial, *Nat. Biotechnol.* **2013**, *31*, 638; e) J. E. Dahlman, C. Barnes, O. F. Khan, A. Thiriot, S. Jhunjunwala, T. E. Shaw, Y. P. Xing, H. B. Sager, G. Sahay, L. Speciner, A. Bader, R. L. Bogorad, H. Yin, T. Racie, Y. Z. Dong, S. Jiang, D. Seedorf, A. Dave, K. S. Sandhu, M. J. Webber, T. Novobrantseva, V. M. Ruda, A. K. R. Lytton-Jean, C. G. Levins, B. Kalish, D. K. Mudge, M. Perez, L. Abezgauz, P. Dutta, L. Smith, K. Charisse, M. W. Kieran, K. Fitzgerald, M. Nahrendorf, D. Danino, R. M. Tuder, U. H. von Andrian, A. Akinc, D. Panigrahy, A. Schroeder, V. Koteliansky, R. Langer, D. G. Anderson, *Nat. Nanotechnol.* **2014**, *9*, 648; f) A. Wittrup, A. Ai, X. Liu, P. Hamar, R. Trifonova, K. Charisse, M. Manoharan, T. Kirchhausen, J. Lieberman, *Nat. Biotechnol.* **2015**, *33*, 870; g) J. Hao, P. Kos, K. Zhou, J. B. Miller, L. Xue, Y. Yan, H. Xiong, S. Elkassih, D. J. Siegwart, *J. Am. Chem. Soc.* **2015**, *137*, 9206; h) Y. Yan, L. Liu, H. Xiong, J. B. Miller, K. Zhou, P. Kos, K. E. Huffman, S. Elkassih, J. W. Norman, R. Carstens, J. Kim, J. D. Minna, D. J. Siegwart, *Proc. Natl. Acad. Sci.USA* **2016**, *113*, E5702.

[17] a) P. Harvie, F. M. Wong, M. B. Bally, *Biophys. J.* **1998**, *75*, 1040; b) W. Li, F. C. Szoka Jr., *Pharm. Res.* **2007**, *24*, 438; c) S. C. Semple, A. Akinc, J. X. Chen, A. P. Sandhu, B. L. Mui, C. K. Cho, D. W. Y. Sah, D. Stebbing, E. J. Crosley, E. Yaworski, I. M. Hafez, J. R. Dorkin, J. Qin, K. Lam, K. G. Rajeev, K. F. Wong, L. B. Jeffs, L. Nechev, M. L. Eisenhardt, M. Jayaraman, M. Kazem, M. A. Maier, M. Srinivasulu, M. J. Weinstein, Q. M. Chen, R. Alvarez, S. A. Barros, S. De, S. K. Klimuk, T. Borland, V. Kosovrasti, W. L. Cantley, Y. K. Tam, M. Manoharan, M. A. Ciufolini, M. A. Tracy, A. de Fougerolles, I. MacLachlan, P. R. Cullis, T. D. Madden, M. J. Hope, *Nat. Biotechnol.* **2010**, *28*, 172; d) X. W. Cheng, R. J. Lee, *Adv. Drug Delivery Rev.* **2016**, *99*, 129.